Available online at www.sciencedirect.com
SCIENCE DIRECT
Thermochimica Acta 441 (2006) 168–175
thermochimica acta
www.elsevier.com/locate/tca

Thermodynamic and morphological analysis of eutectic formation of CBZ-L-Asp and L-PheOMe·HCl mixtures

Hyun Jung Kim, Jong Hoon Kim, Sung Hun Youn, Chul Soo Shin *

Department of Biotechnology, College of Engineering, Yonsei University, 134 Shinchon-Dong, Seodaemun-Gu, Seoul 120-749, South Korea

Received 3 July 2005; received in revised form 30 November 2005; accepted 1 December 2005

Abstract

The eutectic melting of a CBZ-L-Asp/L-PheOMe·HCl model mixture was investigated in kinetic, thermal, thermodynamic, rheological, and morphological aspects. From TX-phase diagrams, the eutectic composition was determined to be 0.55 M fraction of CBZ-L-Asp. The highest melting rate and the lowest apparent viscosity in the range of 55–75 °C were obtained at the eutectic composition. Using Arrhenius plots of melting rates and apparent viscosities, minimum activation energies in the range of 60–80 °C were obtained at the eutectic composition, whereas maximum values were attained below 60 °C. At the eutectic composition, the maximum heat of fusion, the lowest excess free energy, and the highest excess entropy values were observed by differential scanning calorimetry (DSC). A highly homogeneous morphology due to rearrangement of molecules was observed in the eutectic mixture via scanning electron microscopy and X-ray diffraction analysis. IR spectra revealed that hydrogen bonding in the mixture increases during eutectic melting.

Keywords: Eutectic mixture; Activation energy; Enhanced homogeneity; Excess thermodynamic function

1. Introduction

Many bioactive compounds have been developed via biocatalytic reactions. However, since the substrates of reactions in many cases are water-insoluble, non-aqueous organic solvent media have been used instead of aqueous media. In spite of many efforts, low concentration levels (several mM scale) of reaction mixtures are still a bottleneck in industrial biocatalysis, resulting in low volumetric productivity. Therefore, technologies for preparation of high concentration levels of reaction mixtures should be developed.

Eutectic mixture formation is a well-known melting technique. In enzymatic reactions, eutectic formation technique has been used to prepare homogeneous substrate mixtures with extremely high concentration levels [1,2]. Eutectic mixtures of amino acids have mainly been applied for peptide syntheses [3–6]. The liquefied mixtures are easily formed by using some amino acids protected with acetyl (Ac), *tert*-butyloxycarbonyl (Boc), 9-fluorenylmethyloxycarbonyl (Fmoc), and benzyloxycarbonyl (CBZ) groups. The adjuvant, which is added in small amounts (usually 5–30%, w/w), enhances formation of a eutectic mixture [7]. In addition, the eutectic formation mechanism was elucidated by computer-aided molecular dynamics simulation [8].

Eutectic melting has been analyzed with respect to thermal, thermodynamic, and morphological properties [9]. Differential scanning calorimetry (DSC) has been frequently used to determine the thermal properties of a mixture, such as melting point [10], eutectic composition [11], crystallization behavior [12], and heat of fusion [11,13–16]. Based on these properties, excess thermodynamic functions can be calculated and used to determine the optimal conditions of eutectic mixture formation [17,18]. The molecular structures of eutectic mixtures have been analyzed based on morphological characteristics determined by using polarizing, optical [19–21], and scanning electron microscopy [15,21,22]. However, the relationships between those properties have not been fully studied. Kinetic studies of eutectic melting have been investigated at a simple level; however, the major driving forces for eutectic melting have not yet been identified.

In this study, we determined mixtures of CBZ-L-Asp and L-PheOMe·HCl as a model system. These compounds are

* Corresponding author. Tel.: +82 2 2123 2886; fax: +82 2 362 7265.
E-mail address: csshin@yonsei.ac.kr (C.S. Shin).

0040-6031/$ – see front matter © 2005 Elsevier B.V. All rights reserved.
doi:10.1016/j.tca.2005.12.001

substrates of the synthesis of aspartame precursor [3,6] if the free base of L-PheOMe is used. In order to elucidate the characteristics of eutectic melting, kinetic, thermal, thermodynamic, rheological, and morphological properties on the mole fraction of CBZ-L-Asp were analyzed. Based on the comprehensive knowledge of eutectic melting, we can provide some useful information for application of eutectic characteristics to media engineering in biocatalysis.

2. Materials and methods

2.1. Eutectic formation of mixtures

Each compound of CBZ-L-Asp and L-PheOMe·HCl was ground for 10 min in a mortar. Then, the resulting powder was used in eutectic melting. Eutectic mixture of CBZ-L-Asp and L-PheOMe·HCl was prepared by incubating 10 mL screw-top glass vials containing 0.5 mmol of each compound for 30 min in a water bath (Jeio Tech, WB-10M) at 60 °C. On the other hand, annealed solutions were made by repeating the cooling and heating procedures of substrate mixture. Methanol (99.9% purity) was added as an adjuvant in different amounts. The melting points of mixtures CBZ-L-Asp and L-PheOMe·HCl without adjuvant were measured via differential scanning calorimetry (Sinco, DSC S-650), and plotted on a temperature–mole fraction (TX)-diagram. The melting point of mixtures containing methanol adjuvant (20%, w/w) was measured in an oil bath.

2.2. Measurement of melting rates and Arrhenius plots

After various mole fractions of CBZ-L-Asp/L-PheOMe·HCl mixtures were prepared, melting rates were measured in a thermostat water jacket. The total amount of CBZ-L-Asp and L-PheOMe·HCl was set to 1.0 mmol. Methanol was added to the mixtures at 20% (w/w) as an adjuvant. The time for complete melting was then measured, and a melting rate constant was calculated. Activation energies were estimated from Arrhenius plots of logarithmic melting rate versus reciprocal temperature and logarithmic viscosity versus reciprocal temperature.

2.3. Rheological analysis

The total amount of CBZ-L-Asp/L-PheOMe·HCl mixture was set to 30 mmol, and methanol was added at 20% (w/w) to a 50 mL screw-top glass vial. Equilibrated eutectic melts were made by repeating incubation in water baths at 20 and 60 °C. Shear stresses relating to the shear rate of the mixtures were measured at various temperatures using a rheometer (Brookfield, DV-III equipped with a no. 31 spindle) and plotted on the *XY*-axis. Apparent viscosities from the slopes were calculated using the least squares method.

2.4. Thermal analysis

The thermal analyses of mixtures CBZ-L-Asp/L-PheOMe·HCl at various mole fractions were performed using differential scanning calorimetry (Scinco, DSC S-650). After mixtures were ground for 10 min in a mortar, the resultant powders were placed uniformly onto an aluminum pan, then heated from 25 °C to 200 °C at a rate of 5 °C min^{-1} under a nitrogen atmosphere. Three replications per sample were performed to ensure reproducibility.

2.5. Morphological analysis

The morphology both before and after eutectic melting of CBZ-L-Asp/L-PheOMe·HCl mixtures ($X_{CBZ\text{-}L\text{-}Asp}$: 0.55) was analyzed. For eutectic melting, ground CBZ-L-Asp/L-PheOMe·HCl mixtures were mixed with 10% methanol. The mixtures were then incubated for 30 min in a water bath at 60 °C, followed by solidification at room temperature. Resultant microstructures were analyzed on a scanning electron microscope (Hitachi, S2700) both before and after eutectic melting. Annealed eutectic mixtures were solidified to a powder at room temperature and the morphologies of the fracture surfaces of the grains were analyzed.

X-ray diffraction patterns (Rigaku, D/max; Rint 2000) of CBZ-L-Asp/L-PheOMe·HCl mixtures ($X_{CBZ\text{-}L\text{-}Asp}$: 0.55) both before and after annealed eutectic melting were obtained at 30 kV–25 mA and at a scan speed of 4° min^{-1}. These data were plotted as counts versus a 2θ diffraction angle.

2.6. FT-IR spectroscopy

Infrared spectra of CBZ-L-Asp/L-PheOMe·HCl mixtures ($X_{CBZ\text{-}L\text{-}Asp}$: 0.55) both before and after annealed eutectic melting were obtained using FT-IR (BIO RAD, FTS-135). A powder-type of potassium bromide was used as a reference. IR spectra were observed in the wave number range of 400–4000 cm^{-1}.

2.7. Chemicals

N-Benzyloxycarbonyl-L-aspartic acid (CBZ-L-Asp) was purchased from Novabiochem Co. L-Phenylalanine methyl ester hydrochloride (L-PheOMe·HCl) and potassium bromide were products of Sigma Chemical Co. Methanol (HPLC grade) was obtained from Duksan Co.

3. Results

3.1. Thermodynamic analysis of eutectic mixtures

Phase diagrams of the solid–liquid equilibrium for different mole fractions of CBZ-L-Asp/L-PheOMe·HCl mixtures were experimentally constructed using a differential scanning calorimeter. Fig. 1 shows temperature–mole fraction (TX) phase diagrams of mixtures in annealed state. The melting temperature of a mixture varied depending on the solute composition. In the absence of an adjuvant, a eutectic point of 92 °C was attained at 0.55 $X_{CBZ\text{-}L\text{-}Asp}$, which corresponds to a eutectic composition. In the presence of the adjuvant methanol (20%, w/w), the melting curve was shifted to the low side and a eutectic point of 45 °C was attained at the same composition (0.55 $X_{CBZ\text{-}L\text{-}Asp}$, dotted line).

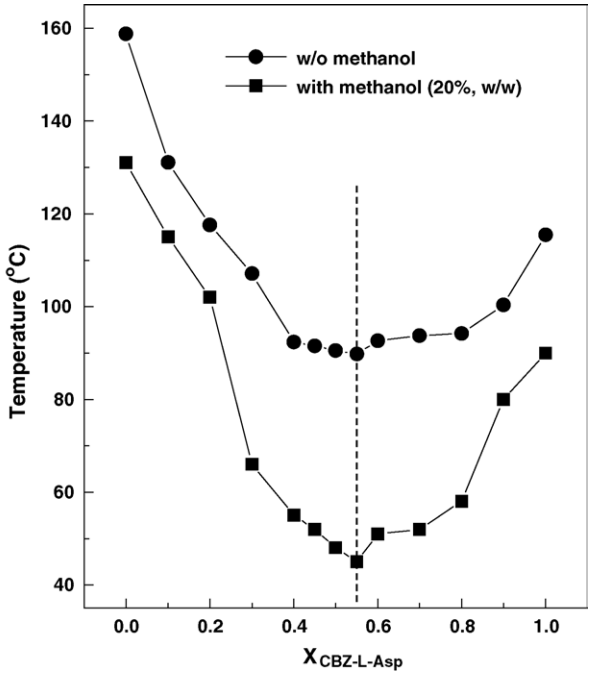

Fig. 1. Temperature–mole fraction (TX) phase diagrams of CBZ-L-Asp/L-PheOMe·HCl mixtures.

The melting rates of CBZ-L-Asp/L-PheOMe·HCl mixtures including 20% (w/w) methanol were measured at CBZ-L-Asp mole fractions of 0.40–0.90. Melting rate constants were calculated using the following equations:

$$S \xrightarrow{k} S' \tag{1}$$

$$v = \frac{dS'}{dt} = k[S] \tag{2}$$

where S, S', and k are the solid mixture, liquid melt, and melting rate constant, respectively. At 70 °C or less, a maximum value of the melting rate was obtained at the eutectic composition (dotted line). Above 70 °C, however, the rate increased gradually with an increasing amount of $X_{CBZ\text{-}L\text{-}Asp}$ with no maximum point (Fig. 2).

From Arrhenius plots of melting rate versus temperature, the activation energy (E_a^m) was estimated at intervals of 10 °C between 50 and 80 °C (Table 1 and Fig. 3). In the region of 60–80 °C (Fig. 3), minimum activation energies were observed at the eutectic composition ($X_{CBZ\text{-}L\text{-}Asp}$: 0.55, dotted line). The E_a^m value increased with distance from the eutectic composition. However, in the low temperature region of 50–60 °C, a maximum value of 122.0 kJ mol^{-1} was obtained at the eutectic composition.

3.2. Rheological analysis of eutectic mixtures

Mixtures CBZ-L-Asp/L-PheOMe·HCl with various mole fractions ($X_{CBZ\text{-}L\text{-}Asp}$: 0.40–0.60) were melted including 20% methanol adjuvant. The shear rates on the shear stress of melts were measured and plotted (Fig. 4), and apparent viscosities were estimated from the slopes of plots (Fig. 5). Apparent viscosity curves of solute mole fraction showed patterns similar

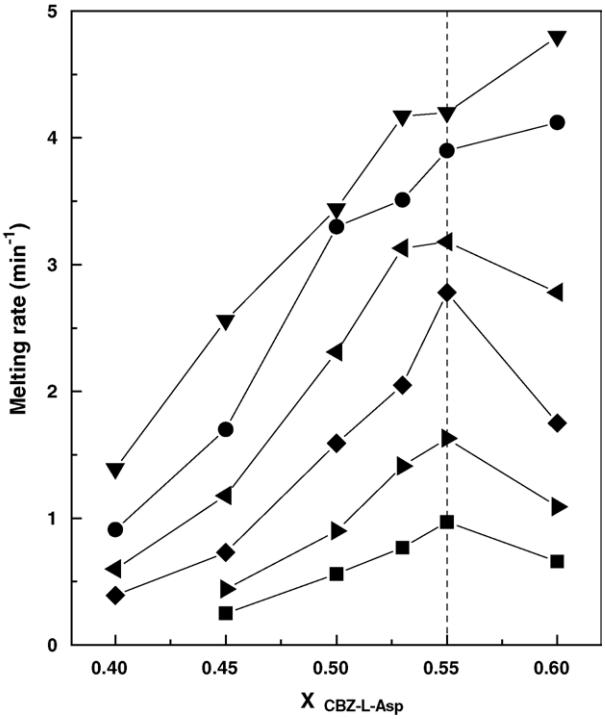

Fig. 2. Melting rates of CBZ-L-Asp/L-PheOMe·HCl mixtures. Methanol was added at 20% (w/w) as an adjuvant: (■) 55 °C; (►) 60 °C; (♦) 65 °C; (◄) 70 °C; (●) 75 °C; (▼) 80 °C.

to melting rates at 50–80 °C. Minimum apparent viscosities were obtained at the eutectic composition ($X_{CBZ\text{-}L\text{-}Asp}$: 0.55). The viscosity increased with distance from the eutectic mole fraction. The lowest minimum apparent viscosity of 0.41 Pa s

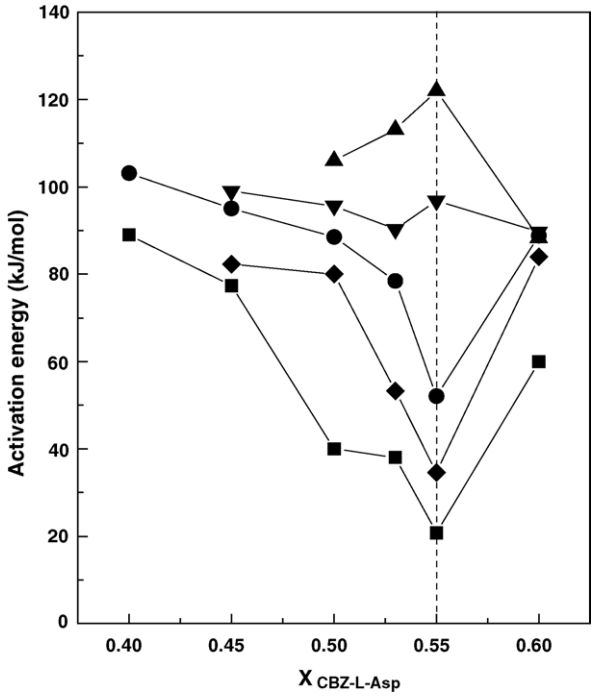

Fig. 3. Activation energies of CBZ-L-Asp/L-PheOMe·HCl mixtures. Methanol was added at 20% (w/w) as an adjuvant: (▲) 50–60 °C; (▼) 55–65 °C; (●) 60–70 °C; (♦) 65–75 °C; (■) 70–80 °C.

Table 1
Melting rates and activation energies in the temperature range 50–80 °C

Temperature (°C)	$X_{CBZ\text{-}L\text{-}Asp}$[a]	Melting rate (min^{-1})	Activation energy ($kJ\,mol^{-1}$)	$X_{CBZ\text{-}L\text{-}Asp}$[a]	Melting rate (min^{-1})	Activation energy ($kJ\,mol^{-1}$)
50	0.40	n.d.	92.04	0.53	0.39	74.94
55		n.d.			0.77	
60		0.20			1.41	
65		0.39			2.05	
70		0.60			3.13	
75		0.91			3.51	
80		1.39			4.17	
50	0.45	n.d.	89.30	0.55[b]	0.42	69.84
55		0.25			0.97	
60		0.44			1.63	
65		0.73			2.78	
70		1.18			3.18	
75		1.70			3.96	
80		2.56			3.97	
50	0.50	0.27	83.65	0.60	0.41	88.79
55		0.56			0.66	
60		0.90			1.09	
65		1.59			1.75	
70		2.31			2.78	
75		3.60			4.12	
80		3.44			5.00	

[a] Mole fraction of CBZ-L-Asp.
[b] Eutectic composition; n.d.: not detected.

was observed at the eutectic composition (dotted line). At 0.40 $X_{CBZ\text{-}L\text{-}Asp}$, the apparent viscosity of the melted mixture at 50 °C was 4.41 times higher than at 80 °C. However, at 0.55 $X_{CBZ\text{-}L\text{-}Asp}$ (the eutectic composition), the value decreased to 1.80 times. At 70 °C or greater, the apparent viscosity did not significantly vary on the mole fraction of CBZ-L-Asp.

Activation energies (E_a^v) based on apparent viscosities were estimated from Arrhenius plots (Fig. 6). The activation energy in the high region of 65–80 °C was smaller than in the low region of 50–65 °C. In the high temperature region, the minimum E_a^v value of 1.81 kJ mol^{-1} was observed at eutectic composition (dotted line). The E_a^v value increased with distance from the eutectic composition. On the other hand, in the low region of 50–65 °C, a maximum value of 45.2 kJ mol^{-1} was observed at eutectic composition. Activation energies obtained from viscosities showed patterns similar to activation energies obtained from melting rates.

3.3. Thermal analysis of eutectic mixtures

Thermal analyses of CBZ-L-Asp/L-PheOMe·HCl mixtures were performed using a DSC. Enthalpies for eutectic melting (ΔH) were estimated and a HX-diagram was constructed (Fig. 7). Thermodynamic functions, excess Gibbs free energy (G^E) values and excess entropy (S^E) values were computed by using the following equations [9]:

$$-\ln x_i^l \gamma_i^l = \frac{\Delta H_i^o}{R}\left(\frac{1}{T} - \frac{1}{T_i^o}\right) \quad (3)$$

$$G^E = RT(x_1 \ln \gamma_1^l + x_2 \ln \gamma_2^l) \quad (4)$$

$$S^E = -R\left(x_1 \ln \gamma_1^l + x_2 \ln \gamma_2^l + x_1 T \frac{\delta \ln \gamma_1^l}{\delta T} + x_2 \frac{\delta \ln \gamma_2^l}{\delta T}\right) \quad (5)$$

where x_i, γ_i^l, ΔH_i^o, and T_i^o are the mole fraction, the activity coefficient, the apparent heat of fusion, and the melting point of the pure component i ($i = 1, 2$), respectively. T is the melting temperature of a binary mixture at x_i. The superscript l indicates the liquid phase of mixtures. As shown in Fig. 7, a maximum fusion enthalpy was obtained at the eutectic composition (dotted line). The fusion enthalpy decreased as $X_{CBZ\text{-}L\text{-}Asp}$ either increased or decreased from the eutectic composition, suggesting that the HX-diagram of a mixture can be used to predict the eutectic composition [11]. An ideal TX-diagram was constructed by substituting $\gamma_i^l = 1$ into Eq. (3). The result was similar to experimental results (data not shown).

Based on the HX-diagram, excess free energy and excess entropy values for each mole fraction were calculated using Eqs. (4) and (5). As shown in Fig. 8, at the eutectic composition (dotted line) a minimum value of −82.6 J mol^{-1} was obtained for excess Gibbs free energy (G^E) whereas a maximum value of 2.3 J mol^{-1} K^{-1} was obtained for excess entropy (S^E).

3.4. Morphological analysis of eutectic mixtures

Morphologies both before and after eutectic melting of CBZ-L-Asp/L-PheOMe·HCl mixtures at eutectic composition were

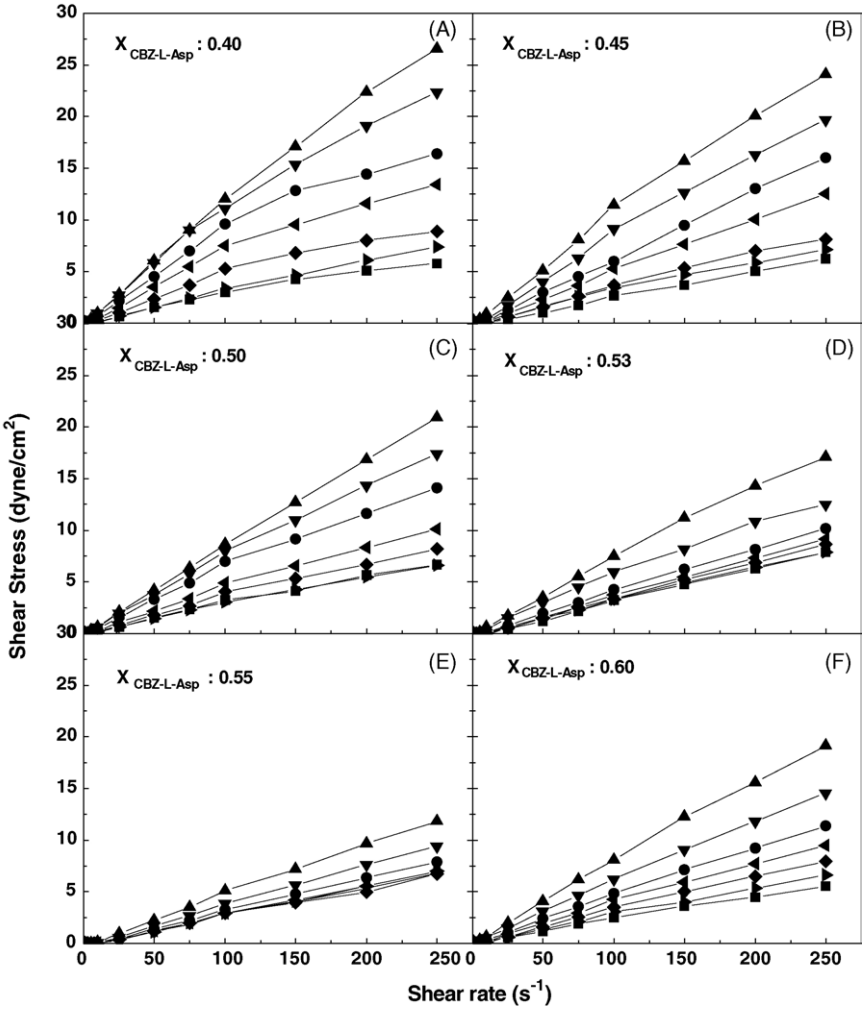

Fig. 4. Plots of the shear stress vs. the shear rate for melted CBZ-L-Asp/L-PheOMe·HCl mixtures. Methanol was added at 20% (w/w) as an adjuvant: (▲) 50 °C; (▼) 55 °C; (●) 60 °C; (◄) 65 °C; (♦) 70 °C; (►) 75 °C; (■) 80 °C.

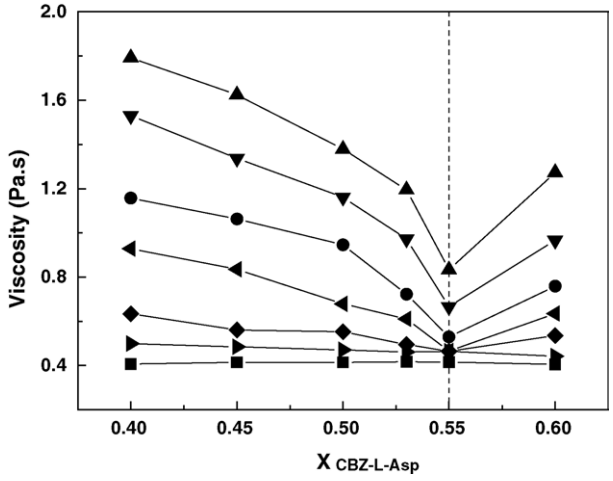

Fig. 5. Apparent viscosities of melted CBZ-L-Asp/L-PheOMe·HCl mixtures. Methanol was added at 20% (w/w) as an adjuvant: (▲) 50 °C; (▼) 55 °C; (●) 60 °C; (◄) 65 °C; (♦) 70 °C; (►) 75 °C; (■) 80 °C.

analyzed using the scanning electron microscopy (SEM). The snapshots of SEM morphologies for the mixture before and after eutectic melting were obtained (Fig. 9). In a mixture before the eutectic melting, it exhibited various shapes of sharp crystals among which were large sizes (Fig. 9, before). On the contrary, the annealed eutectic mixture after heat treatment exhibited homogeneous and similar shapes with smooth edges (Fig. 9, after).

Homogeneities of mixtures before and after eutectic melting of CBZ-L-Asp/L-PheOMe·HCl were analyzed at the molecular level based on X-ray diffraction (XRD) patterns. In a mixture before eutectic melting, a noisy base line with intermittent irregular peaks was observed (Fig. 10, before). On the other hand, for the re-solidified eutectic mixture obtained after eutectic melting, a base line with relatively little noise and similar peak heights at regular intervals was observed (Fig. 10, after). Comparison of the peaks showed that the eutectic mixture is highly homogeneous compared to the mixture before heat treatment.

When hydrogen bonds are formed in a mixture, infrared (IR) spectral bands are generally shifted to a low wave number and the bands are broadened [21,24]. After eutectic melting, IR spec-

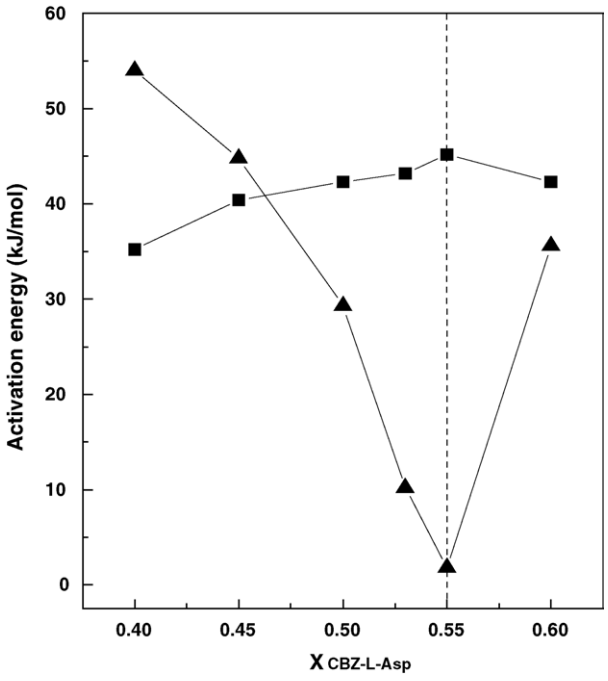

Fig. 6. Activation energies of the apparent viscosities of CBZ-L-Asp/L-PheOMe·HCl mixtures. Methanol was added at 20% (w/w) as an adjuvant: (■) 50–65 °C; (▲) 65–80 °C.

tra of mixtures showed bands shifted to low wave number and broadened (Fig. 11). Thus, strong hydrogen bonds between the molecules of eutectic mixtures were present. Due to hydrogen bonds between the C=O groups and the OH-groups of eutectic mixtures, the IR peaks were shifted from 1713.6 to 1705.9 cm^{-1}, and from 1752.2 to 1748.3 cm^{-1}, and strong band broadenings occurred.

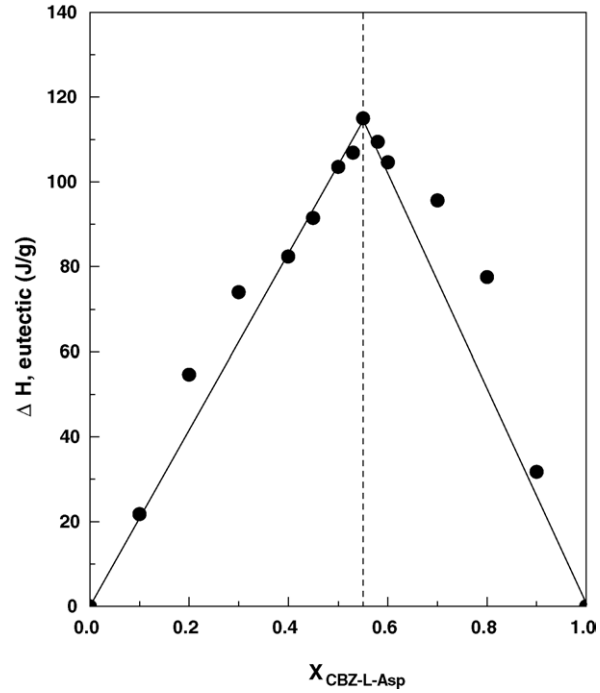

Fig. 7. An HX-diagram for CBZ-L-Asp/L-PheOMe·HCl mixtures.

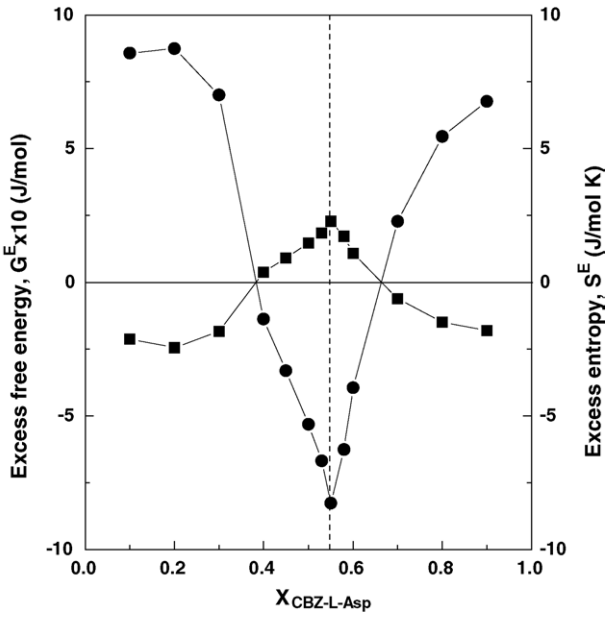

Fig. 8. Excess thermodynamic functions for CBZ-L-Asp/L-PheOMe·HCl mixtures: (●) G^E; (■) S^E.

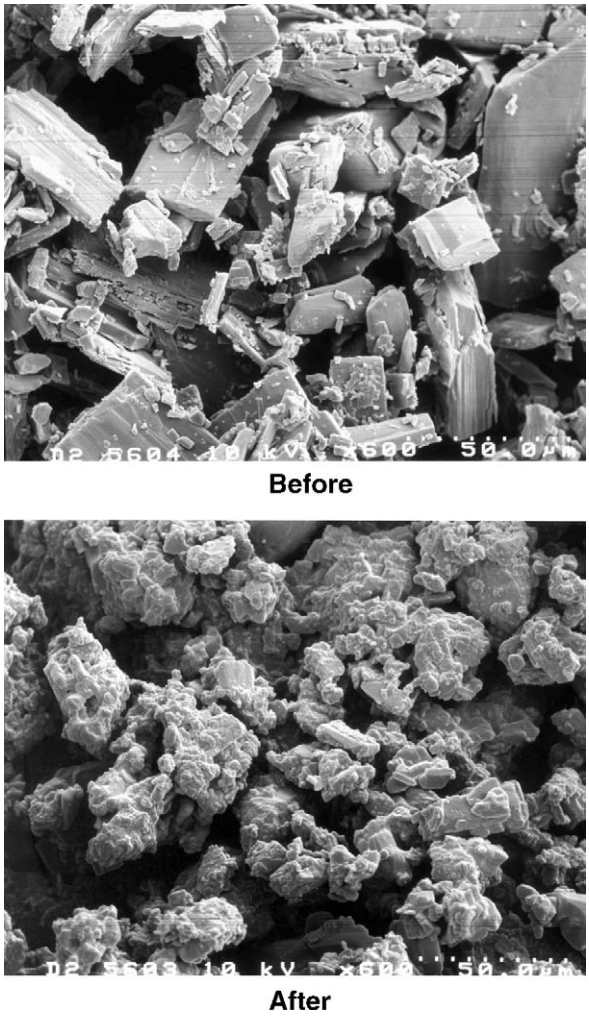

Fig. 9. Scanning electron microscope (SEM) photomicrographs before and after eutectic formation. Methanol was added at 10% (w/w) as an adjuvant.

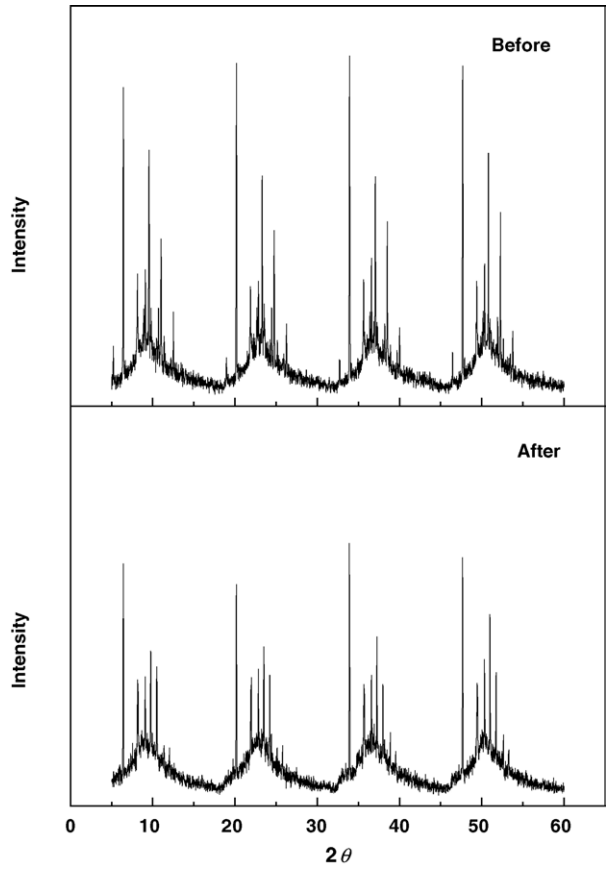

Fig. 10. X-ray diffraction (XRD) patterns before and after eutectic formation.

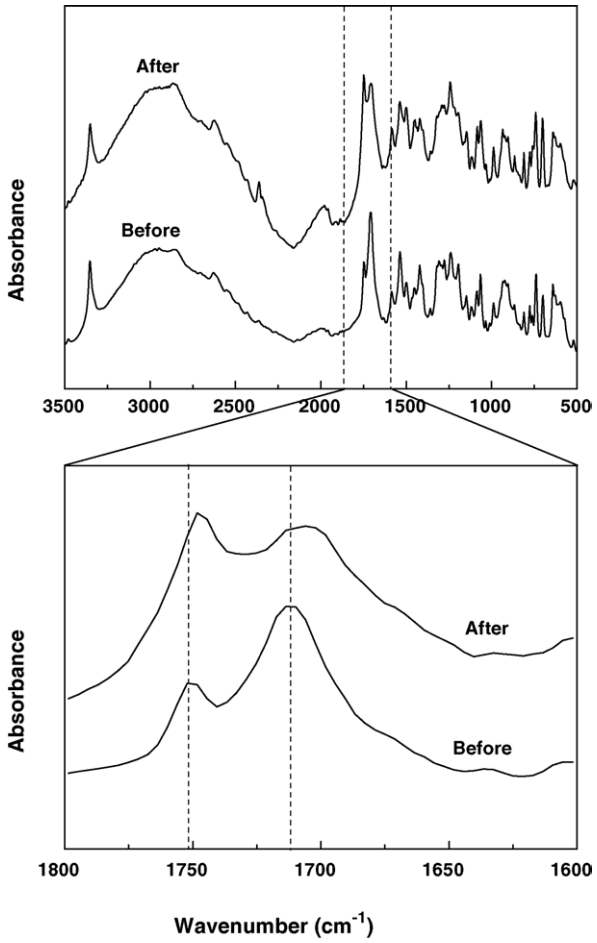

Fig. 11. IR spectra before and after eutectic formation.

4. Discussion

The phase change of a heterogeneous solid mixture to a homogeneous liquid, called melting, occurs via uniform rearrangement of different molecules. According to our experimental results, kinetic, thermal, thermodynamic, and rheological properties are changed significantly at the eutectic composition. Maximum melting rates were attained at the eutectic composition except in very high temperature regions (Fig. 2), indicating that interactions between the molecules of a binary mixture at the eutectic composition are relatively accelerated, resulting in rapid rearrangement of molecules. Minimum E_a^m values at temperatures above 60 °C were also observed at the eutectic composition (Fig. 3), suggesting that the conditions most favorable for formation of the homogeneous phase can be established at that composition. Below 60 °C, the maximum E_a^m values were attained at the eutectic composition. It was considered that numerous intermolecular interactions occur between solid molecules with the aid of solvent adjuvant near the eutectic point. It was considered that maximum molecular cluster arrays are generated and many molecular interactions are required for the breakup of clusters.

Hereafter, it is necessary to distinguish the solubilizing effect of adjuvant from its melting–stimulating effect. Although there is no clear criterion to differentiate them, it can be easily estimated whether the mixture can form a homogeneous solution under addition of solvent or not. The actual effect of adding adjuvant as a eutectic modifier was well described in some references [1,7].

The eutectic melting phenomenon was also analyzed using the heat of fusion values for the mixture of various mole fractions. The HX-diagram (Fig. 7) shows the portion of the eutectic melt at the mole fraction. The maximum eutectic portion can be attained at the eutectic composition. In non-eutectic compositions, a certain part of the component is engaged in eutectic melting whereas the rest remains in a pure form without melting. Thus, extra thermal energy is required for complete melting of the mixture. Hence, the high melting temperatures required for non-eutectic compositions can be explained.

During the melting process of a binary mixture, the lowest excess Gibbs free energy (G^E) value and the highest excess entropy value (S^E) were obtained at the eutectic composition (Fig. 8), suggesting that these thermodynamic terms can be used as an indicator of eutectic melting. Under ideal conditions, i.e. $\gamma_i^l = 1$, the excess values will be zero. Therefore, the negative differences between real and ideal excess Gibbs free energies indicate that extra energy will increase the kinetic energy of a homogeneous liquid melt. Besides, the maximum S^E value observed at the eutectic composition confirms that rearrangement of molecules of the mixture occurs actively at that composition.

The minimum activation energy (E_a^v) calculated from the viscosity was obtained at the eutectic composition (Fig. 6), indicating that high molecular kinetic energies can be maintained at that composition. In other words, a high rate of molecular interaction at the eutectic composition can induce fast melting, resulting in generation of maximum extra energy. This extra energy can be converted to the kinetic energy of molecules, thus lowering the viscosity of the mixture. However, the maximum E_a^v value was obtained at the eutectic composition, probably due to the extent of viscous natures in melts was relatively high at low temperatures. This high viscosity can induce strong intermolecular interactions. Similar results have been discussed by Sharma [23]. This fact can be confirmed from a morphological change before and after melting at the eutectic composition (Figs. 9 and 10), revealing that a homogeneous annealed mixture is formed from a heterogeneous mixture by eutectic melting.

In case of molecular mixtures, IR spectra can be changed by the extent of H-bond forming moiety, the mole fraction of substances, and the kind and quantity of adjuvant, respectively. Therefore, if the mole fraction of a component and the kind of adjuvant are determined, the IR spectra will vary, depending only on whether the eutectic mixture formation occurred or not in our model mixture. Preliminarily, we confirmed that the IR spectra of pure CBZ-L-Asp and L-PheOMe·HCl do not change by the melting and crystallizing process of each molecule (data not shown).

5. Conclusion

The lowest melting temperature of a mixture is obtained at the eutectic composition, probably caused by rapid homogeneous rearrangement of molecules due to active interactions between the molecules. Changes in the melting rate, activation energy, excess thermodynamic function, and viscosity are apparently responsible for this phenomenon. Our investigation can provide some useful information for application of eutectic characteristics to media engineering in biocatalysis.

References

[1] I. Gill, E. Vulfson, Trends Biotechnol. 12 (1994) 118–122.
[2] H.J. Kim, S.H. Youn, C.S. Shin, J. Biotechnol., in press.
[3] I. Gill, R. López-Fandiño, X. Jorba, E.N. Vulfson, Enzyme Microb. Technol. 18 (1996) 162–183.
[4] C. Kim, C.S. Shin, Enzyme Microb. Technol. 28 (2001) 611–616.
[5] R. López-Fandiño, I. Gill, E.N. Vulfson, Biotechnol. Bioeng. 43 (1994) 1024–1030.
[6] J.E. Ahn, C. Kim, C.S. Shin, Process Biochem. 37 (2001) 279–285.
[7] R. López-Fandiño, I. Gill, E.N. Vulfson, Biotechnol. Bioeng. 43 (1994) 1016–1023.
[8] H.J. Kim, J.H. Kim, S.H. Youn, C.S. Shin, Biotechnol. Prog. 21 (2005) 1307–1314.
[9] U.S. Rai, R.N. Rai, J. Therm. Anal. 53 (1998) 883–893.
[10] C.-C. Huang, Y.-P. Chen, Chem. Eng. Sci. 55 (2000) 3175–3185.
[11] Z.-R. Liu, Y.-H. Shao, C.-M. Yin, Y.-H. Kong, Thermochim. Acta 250 (1995) 65–76.
[12] C.C. Gryte, H. Berghmans, G. Smets, J. Polym. Sci. Pol. Phys. 17 (1979) 1295–1305.
[13] C.-M. Yin, Z.-R. Liu, Y.-H. Kong, C.-L. Jia, X.-M. Guo, Thermochim. Acta 262 (1995) 185–193.
[14] C.-M. Yin, Z.-R. Liu, Y.-H. Shao, Y.-H. Kong, Thermochim. Acta 250 (1995) 77–83.
[15] N. Passerini, B. Albertini, M.L. González-Rodríguez, C. Cavallari, L. Rodriguez, Eur. J. Pharm. Sci. 15 (2002) 71–78.
[16] S. Schmid, C.C. Müller-Goymann, P.C. Schmidt, Int. J. Pharm. 197 (2000) 35–39.
[17] B.L. Sharma, N.K. Sharma, M. Rambal, Thermochim. Acta 206 (1992) 71–84.
[18] B.L. Sharma, R. Kant, R. Sharma, S. Tandon, Mater. Chem. Phys. 82 (2003) 216–224.
[19] R.P. Rastogi, P.S. Bassi, J. Phys. Chem. 68 (1964) 2398–2406.
[20] B.L. Sharma, N.K. Sharma, P.S. Bassi, J. Cryst. Growth 67 (1984) 633–638.
[21] X. Zhu, Y. Xiao, P. He, D. Yan, Y. Fang, Polym. Int. 52 (2003) 813–818.
[22] R.J.M. Zwiers, S. Gogolewski, A.J. Pennings, Polymer 24 (1983) 167–174.
[23] B.L. Sharma, Mater. Sci. Eng. B25 (1994) 11–19.
[24] P.W. Stott, A.C. Williams, B.W. Barry, J. Control. Release 50 (1998) 297–308.